Investigation of plasma-in-liquid induced copper oxidation

Bachelor Thesis

in the
Degree Program
„Bachelor of Science“
in Physics

at the Faculty of Physics and Astronomy
of the Ruhr-Universität Bochum

by
Sven Weller

from
Witten

Bochum (2024)

Abstract

The thought of converting CO_2 into chemical energy with green energy exists for a long time, but the large scale implementation is still challenging. The discovery of the CO_2 reduction reaction with a copper catalyst and an electrolyte enables a new possibility of realization. Studies showed, that this reaction is adjustable, if you create nanoparticles on the surface of the catalyst. The problem with this variant is the limited life time and the complicated steps of nanoparticle production. It was discovered that the treatment of copper surfaces with plasma activated water leads to the creation of nanoparticles. This led to the idea of integrating an electrode into the electrolysis setup to ignite a plasma and recreate the nanoparticle. For this reason, this work investigated the behavior of thin copper layers within an electrolyte when a plasma is ignited next to them. In addition, the dissipated energy into the plasma was measured for different electrolytes and working times. The change of the samples was measured via reflective Fourier transformed infrared spectroscopy. The Copper(II)-oxide bond was analyzed. The other copper bonds were to close to the edge or outside the range of the detector. The energy measurements showed a small increase in the dissipated energy for an increase in the concentration. A longer plasma time causes a reduction of the dissipated energy per plasma pulse. Positive and negative voltages had no visible influence on the dissipated energy. After that the change of the copper(II)-oxide was analyzed. First the influence of different voltages was examined. The used electrolyte was distilled water. The results showed overall a reduction of the copper(II)-oxide bond, but only a small influence of the applied voltage was visible. The negative voltages initially had a slower rate of reduction than the positive voltages but catched up later. After that the electrolyte was varied and the applied voltage was kept at negative and positive 20 kV. The results showed first a decrease in the copper reduction with an increase in the KOH concentration. However, later measurements contradict this assumption. Nonetheless it is clearly visible that the positive voltages lead to a larger reduction compared to the negative voltages. At the end, the reduction rates in a measurement series without igniting a plasma was compared to the earlier ones. This showed a drastically increase in reduction rate when the plasma is not ignited. One series showed saturation. This was also predicted for earlier measurements but did not occur. If the ignition of the plasma creates other copper bonds that will not form without the plasma is not visible from this work and may be an interesting topic for the future.

Zusammenfassung

Der Gedanke CO_2 mittels erneuerbarem Strom in chemische Energie zu wandeln und damit Energie zu speichern ist schon länger vorhanden, aber die großflächige Umsetztung verursachte bisher immer Probleme. Die Entdeckung der CO_2 Reduktionsreaktion mit einem Kupferkatalysator und einem Elektrolyt erschaffte eine neue Möglichkeit der Umsetzung. Studien zeigten, dass genau diese Reaktion verbessert werden kann, wenn man Nanopartikel als Katalysator verwendet. Das Problem bei dieser Variante ist jedoch die begrenzte Arbeitszeit und der komplizierte Herstellungsprozess der Katalysatornanopartikel. Es wurde festgestellt, dass das Behandeln von Kupferoberflächen mit Plasma aktiviertem Wasser dazu beiträgt Nanopartikel zu erzeugen. Dadurch enstand der Gedanke, in den Aufbau für die CO_2 Reduktion eine Elektrode zur Plasmaerzeugung einzubauen, um damit die Nanopartikel herzustellen. Deshalb wurde in dieser Arbeit untersucht wie sich dünne Kupferschichten innerhalb eines Elektrolyt verhalten, wenn man neben ihnen ein Plasme zündet. Außerdem wurde die im Plasma dissipierte Energie gemessen für verschiedene Elektrolyte und Behandlungszeiten. Die Veränderung der Proben wurde via reflektiver FTIR gemessen. Die Kupfer(II)-Oxid Verbindung wurde analysiert. Andere Kupferverbindungen wurden nicht gemessen, da sie sich außerhalb oder zu nah am Rand des Messbereiches des Detektors befinden. Als erstes wurde die dissipierte Energie analysiert. Die Messungen zeigten eine leichte Steigerung der dissipierten Energie bei einer Erhöhung der KOH Konzentration und eine erhöhte Betriebszeit des Plasmas sorgte für eine geringere dissipierte Energie. Positive und negative Spannungen hatten keinen sichtbaren Einfluss auf die dissipierte Energie. Danach wurde die Veränderung des Kupfer(II)-oxidpeaks analysiert. Zuerst wurde der Einfluss von verschiedenen Spannungen untersucht. Der Elektrolyt war während diesen Messungen destiliertes Wasser. Die Ergebnisse zeigten allgemein eine Reduktion von den Kupfer(II)-oxid, aber nur ein kleiner Einfluss von der Spannung war sichtbar. Die negativen Spannungen hatten eine langsamere Reduktion am Anfang, nahmen aber mit der Zeit wieder zu. Danach wurde der Elektrolyt variiert und die angelegte Spannung blieb bei 20kV. Die Ergebnisse zeigten zuerst eine Abnahme in der Reduktion bei steigender KOH Konzentration an. Spätere Messungen jedoch widersprechen dieser Annahme. Es ist aber deutlich zu sehen, dass positive Spannungen eine höhere Abbaurate haben als negative. Am Ende wurde die Abbaurate von den Messreihen mit dem gezündeten Plasma verglichen mit der Abbaurate von den Proben, die nur im Elektrolyt liegen. Dies zeigte eine deutlich höhere Abbaurate wenn das Plasma nicht gezündet wurde. Außerdem zeigt eine Messung, dass eine Sättigung eintritt, die auch vorher schon vermuted wurde, aber nicht sichtbar war. Ob durch die Zündung eines Plasmas andere Kupferbindungen entstehen wurde nicht sichtbar durch diese Arbeit, ist aber ein interresantes Thema für die Zukunft.

Contents

1 Introduction

Electrochemical CO_2 reduction by copper nanoparticle was introduced years ago, with the promising potential to convert green energy into a chemical energy, and also to produce ethanol, methanol and other carbon bonds from CO_2 and electricity. Recently, a lot of research has been evolving around this method of CO_2 reduction[1][2]. While the said method seems to have a high value in today's time, the production of the catalyst, which is the main component of this method, is rather difficult [3][4] and the lifetime of the nanoparticles, which allow the CO_2 reduction to happen, is only a few working hours [5]. The efficiency and selectivity of the nanoparticle is still a topic of research and a promising aspect on tuning the CO_2 reduction reaction[6]. There are different ways to produce the catalysts, but they all involve the creation of copper nanoparticles on the surface. Pottkämper et al. discovered that treating copper surfaces with plasma activated water (PAW) can also lead to the creation of copper nanoparticles on a surface[7]. The exact type of plasma activated water that can create these nanoparticles is still under investigation. One type of plasma where such particles are created is the nanosecond pulsed plasma in liquids, with a pulse time in the nanosecond range, it is possible to create a plasma while still in the liquid state[8]. This distinguishes this method from other types of plasma that are more commonly used to create plasma-activated water, such as a bubbler system or an arc discharge[9] [10]. From the discovery ability to create nanoparticles with PAW, the idea emerged whether one can integrate an electrode for plasma creation into the setup for CO_2 reduction. With this electrode, a plasma can be ignited to create PAW right next to the copper electrode, which can then interact with the PAW and create these nanoparticles. The interaction of copper and the plasma ignition right next to it will be analyzed in this work with the influence of different electrolytes.

1.1 Aim

The aim of this thesis is to analyze the interaction between PAW and a copper surface. The parameters variation to analyze the oxidation or reduction are the applied voltage of the plasma, the number of total ignited plasma pulses and the electrolyte in which the plasma is ignited. While the main focus is to compare the rate of modification of the copper for different parameters, the energy dissipated into the plasma is also measured for the different solutions. The oxidation or reduction of copper is measured while the voltage applied to the plasma is varied for water, and the liquid is also changed to a Kaliumhydroxide(KOH) solution to measure its influence. The main measurements will be done with a reflective difference FTIR measurement. It is postulated that treatment time, electrolyte and the applied voltage have an impact on the copper oxidation state.

2 Theoretical Background

2.1 Plasma in Liquids

Plasma physics and plasma chemistry is a very broad subject and each plasma has its own unique characteristics. Many parameters influence the type of plasma, such as the pressure, the applied voltage and the medium in which the ignition takes place. This experiment will use an in-liquid plasma, which can also be divided into different categories. Such plasmas are often used to produce plasma activated water or liquids (PAW/PAL). The more common setups use a bubbler, an arc discharge or a gas discharge which is aimed onto the liquid. The bubbler creates gas bubbles that allow the plasmas to ignite inside, while the arc discharge creates an arc between the electrodes and generates a current flow. The gas discharge makes use of the flow of the carrier gas, which transports the plasma particles into the liquid. The setup used in this experiment is a pulsed plasma discharge. Two electrodes are placed in the liquid and then a short voltage pulse in the range of nanoseconds is applied. This will not form an arc, but allow a plasma to be ignited from the liquid state.

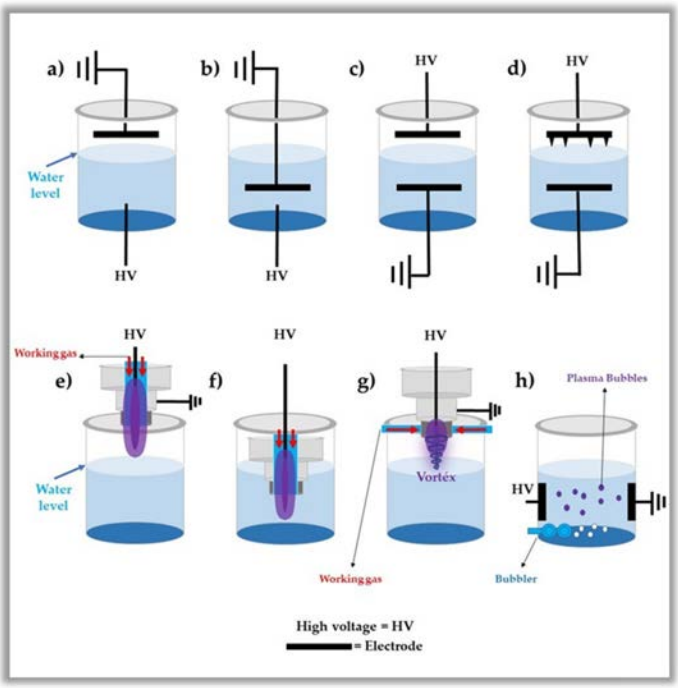

Figure 1: Schematic drawing of different discharges used for the preparation of plasma-activated water (a–c) direct discharge into the water and (d) direct discharge into the water with multi electrodes; (e) discharge in the gaseous phase onto the water surface; (f) discharge in the gaseous phase into the water; (g) discharge in the gas phase onto the water surface with plasma generated on forward vortex flow reactor (FVFR); (h) discharges in bubbles into the water[9]. Setup (b) is used in this experiment

Pulsed discharges in liquids can also be categorized again because the ignition mechanism differs for different pulse lengths. Mainly, these discharges can be divided into microsecond discharges and nanosecond discharges. While the microsecond discharge produces air bubbles around the electrode, where the plasma is then ignited, the nanosecond plasma ignites directly in the liquid state without producing any air bubbles first[8][11]. The nanosecond discharge is used in this experiment and is described in more detail below.

2.1.1 Nanosecond pulsed Plasma discharge

The nanosecond pulsed plasma is ignited directly from the liquid state. This requires a very high electric field and very short pulse rise times in the nanosecond range. The dynamics of this discharge is still not fully understood and is still the subject of many studies. One of the most common theories is ignition by field effects and nanovoids. For these field effects to occur, the electric field must be of high magnitude. A high electric field requires a high applied voltage and a high curvature of the electrode tip. The higher the curvature, the higher the electric field emitted. For this reason, a very small tungsten wire(0,05 mm) is used as the electrode tip, which is cut at an angle at the bottom to create a sharp edge. An example of this electric field is shown below:

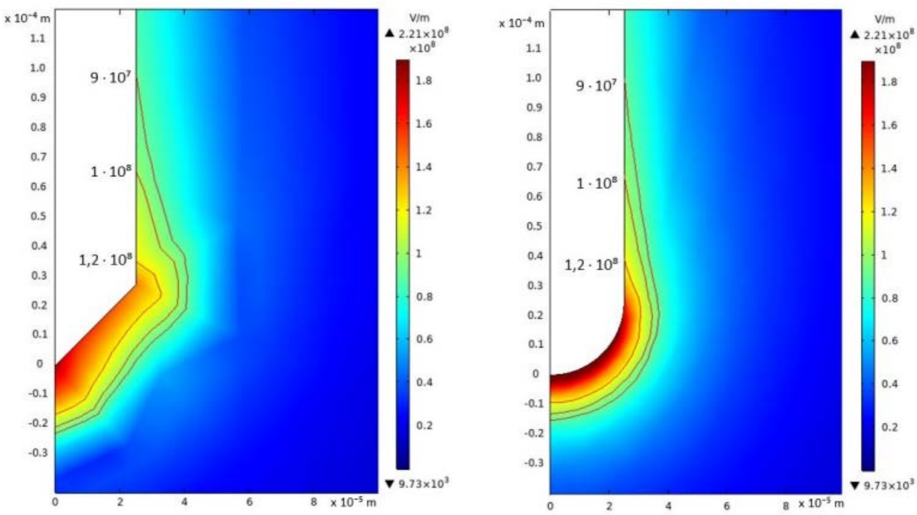

Figure 2: Simulation of an E-field around a wire tip. Done by Oliver Krettek[12]

The positive voltage creates a high electric field, which allows the electrons in the water molecule to tunnel to the electrode tip. This is the principle of field ionization. The negative voltage creates such an electric field that the electrons can leave the electrode tip and get accelerated into the liquid. This is the principle of field emission. As these effects only occur at high electric fields, the conductivity of the liquid plays an important role. The higher the conductivity, the more difficult the plasma ignition becomes, as the increased conductivity allows the current to flow through the liquid and the electric field will not be high enough to reach the required values.

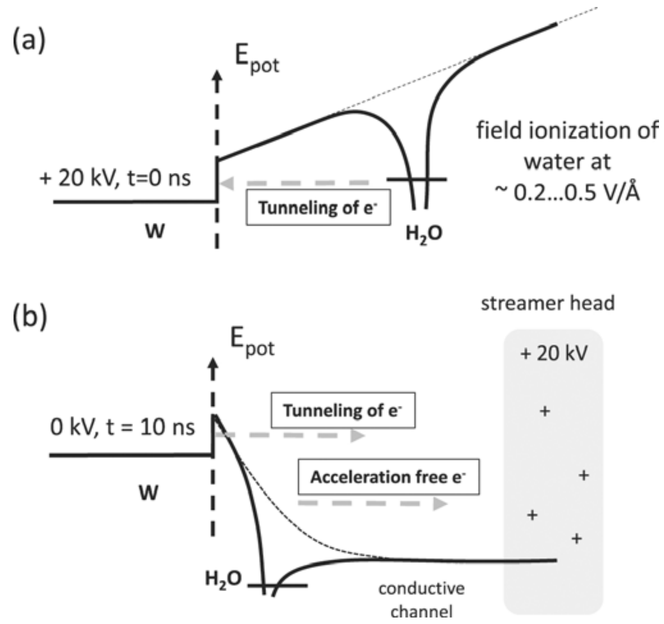

Figure 3: Sketch of field ionization for positive potential between electrode and surrounding as at the beginning of the pulse (a) and field emission for negative potential between electrode and surrounding at the end of the pulse (b)(Grosse et al[11])

The electrons that tunnel into or get emitted by the electrode tip create really high temperatures. As normally the required electric field is only achieved in the area of ignition, the heat is concentrated at that point, which creates a hot spot. This hotspot can reach temperatures of 6000–8000 K. These high temperatures evaporate normal metals. This is why the chosen material of the electrode is tungsten, which boiling temperature is normally somewhere near 5828 K, but with the existing pressure can reach a boiling temperature of 8189 K[11]. Grosse et al.[13] and Krettek et al.[12] investigated the behavior of this electrode tip and discovered that indeed the tip reaches the boiling temperature at the hot spot, but only in a small region at the tip. This creates a crater like structure on the tip, which luckily has a strong enough curvature to reignite the plasma. This mechanic allows to ignite many plasmas with the same electrode, without the need to replace said electrode for some time. This method is the creation of the initial electrons, while the typical streamer like propagation of a plasma has two theories. First is the propagation via field effects, where electrons tunnel between water molecules, and the other is via nanovoids. These are postulated to be small ruptures inside the liquid with very low density, which allow the lose electrons to accelerate and build up the energy to ionize the next water molecule[14]. All of this then forms the discharge in this experiment. The form of this discharge can be compared to a streamer discharge in gas phase plasmas. The main plasma bulk creates

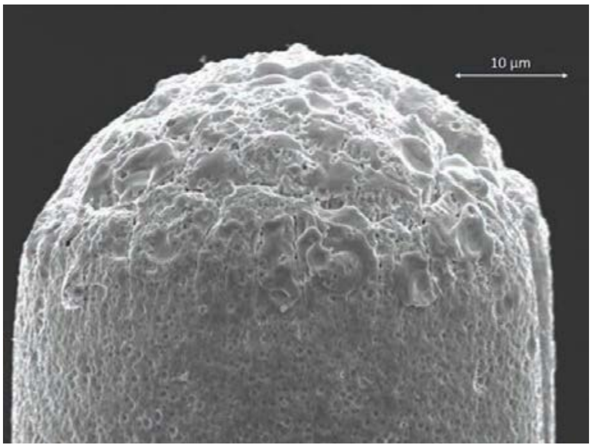

Figure 4: SEM Image of an treated tungsten electrode. The treatment time was 3h at +20 kV with 15 Hz(Krettek et al[12])

streamers, which travel individually through the liquid. Grosse et al.[8] analyzed the expansion of these type of plasmas and took shadowgraphy images. In these you can clearly see the streamers that form. The typical extension of this plasma are a few micrometers.

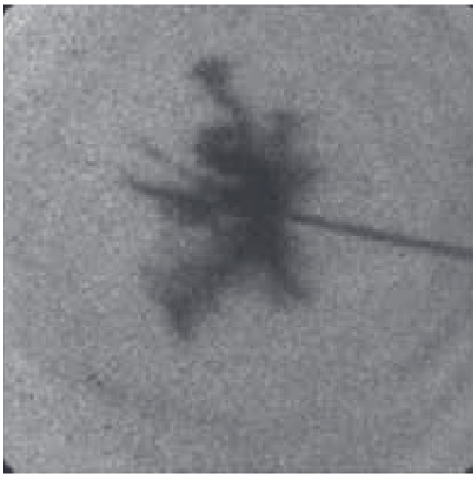

Figure 5: Shadowgraph of bubble expansion at 1 μs for 22 kV applied voltage. The dark region to the right is the shadow of the tungsten wire.(K. Grosse et al [8])

The chemical properties of such plasma ignition differs strongly compared to the other ignitions like in microsecond pulsed plasmas. Chauvet et al. [15] discovered that the H_2O_2 concentration created by nanosecond pulsed plasmas is higher than others. As this plasma is ignited in the liquid phase, the concentration of the created reactive species vary drastically from gas phase plasma. The reactive species, such as O, O_2, OH, H_2, H_2O_2, from this plasma is what allows the copper to form these wanted nanoparticles. Whether microsecond pulsed plasma also create such nanoparticles is still an open question. The leading theory right now behind the nanoparticles production is that the created OH reacts with the copper surface and synthesis Cu_2O nanocrystals.

However it has not been established if only OH is the main driving force or if other species influence the process.

2.2 Synthesis of copper nanoparticles

The synthesis of the PAW produced nanoparticles is comparable with the electrochemical synthesis of copper oxide particles[16],[7]. The synthesis can be divided into 2 parts. In the first part the copper surface interacts with the positive charged particles inside the plasma activated liquid, which absorb an electron and dissolves the copper into the liquid as Cu^{2+} [1].

$$Cu^{+} - e^{-} \longrightarrow Cu^{2+} \tag{1}$$

Inside the liquid the Cu^{2+} reacts with the present $(OH)^{-}$ or H_2O_2 and forms $Cu(OH)_2$ [2,3].

$$Cu^{2+} + 2\,OH^{-} \longrightarrow Cu(OH)_2 \tag{2}$$

$$Cu^{2+} + H_2O_2 + 2\,e^{-} \longrightarrow Cu(OH)_2 \tag{3}$$

After that the second part begins, where the $Cu(OH)_2$ starts to crystallize and form Cu_2O nanoparticle, which then can precipitate onto the surface [4].

$$2\,Cu(OH)_2 + X \longrightarrow Cu_2O + 2\,H_2O + OX \tag{4}$$

The X stands for the plasma created species that can absorb the oxygen, likeH_2. Another reaction that can take place in a water-based solution is water decomposition, which converts the Cu^{2+} with $(OH)^{-}$ directly into CuO and H_2O [5].

$$Cu^{2+} + 2\,OH^{-} \longrightarrow CuO + H_2O \tag{5}$$

Here is to say that the first part of the synthesis happens faster then the second part.

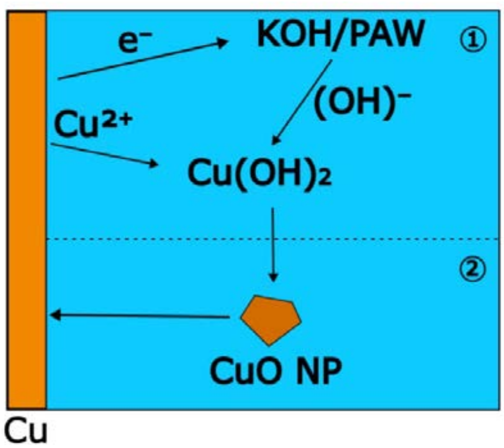

Figure 6: Sketch of the anodic dissolution and the copper nanoparticle crystallization

3 Setup & Measurements

In this chapter the experimental setup and the types of measurements will be described. All measurements were taken at the same setup and it was made sure to have the same parameters.

3.1 Setup

3.1.1 Sample

The sample consists of a silicon oxide wafer made by Si-Mat, where a thin copper layer is deposited on. A sketch of the sample is shown in Figure 7. The wafer consists of a 525 μm thick silicon wafer and both sides are coated by a layer of 1000 nm silicon dioxide(SiO_2). One side of the sample is coated with 10 nm copper, which is done by a high power impulse magnetron sputtering chamber or short HiPIMPS. The wafer is cut into 2 cm x 3 cm pieces, so they fit into the HiPIMPS chamber and into the sample holder of the plasma chamber. Every sample for this measurement had the same properties.

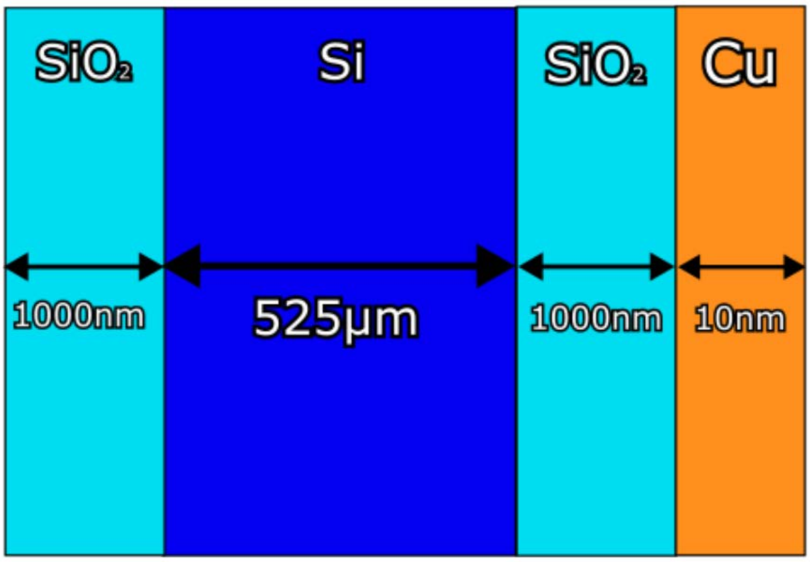

Figure 7: Sketch of a sample. Not to scale

3.1.2 Plasma Chamber

The plasma chamber consists of the main chamber with a circular hole, 4 tube lines to fill the chamber with a liquid, the 2 electrodes and the sample holder. One side of the main chamber is open to place the sample holder. The sample holder consists of 2 round plates, so the sample can be placed between them and can be secured. The sample holder is secured with screws on the plasma chamber. The electrodes are placed inside the tube lines in a pin-to-pin configuration to reach the inside of the main chamber. A sketch of the reactor is displayed in figure 8.

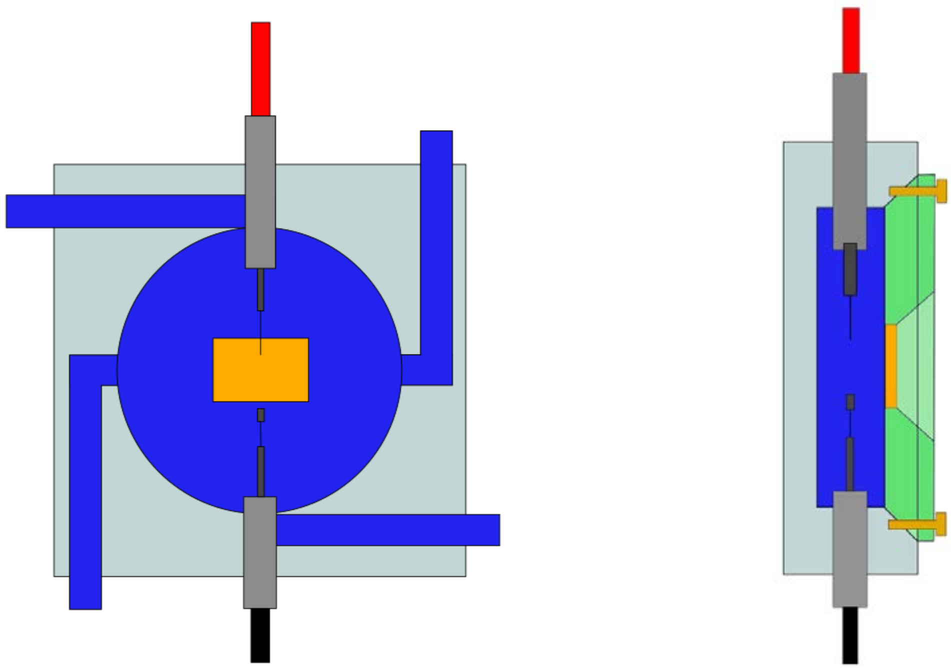

(a) (b)

Figure 8: Sketches of: (a) The front view of the plasma chamber, (b) The side view of the plasma chamber

3.1.3 Measurement Setup

A sketch of the setup is displayed in figure 9. For the FTIR measurements the FTIR spectrometer, Bruker IFS 25/55, is place on the left and with mirrors the emitted IR wave beam is guided on the sample inside the plasma chamber. There the beam is reflected on the second mirror and into the detector. This detector is connected to the FTIR spectrometer and needs to be cooled down with liquid nitrogen. The detector takes some time to reach the desired temperature, so it was cooled for half an hour to an hour before each series of measurements. Also the FTIR spectrometer is connected to a PC to display the measurements while they are taken. The plasma is powered by an nanosecond high voltage pulser, the FPG 30-01NK10-NEG for negative voltages and the FPG 30-01NK10 for positive voltages from FID GmbH. This pulser is connected to the plasma chamber with a 12 meter long cable and an integrated back current shunt to measure the voltage and current. For the energy measurements there was no need for the FTIR but an oscilloscope, the HDO6104A from Teledyne LeCroy, is connected with the 12 meter long cable to get the voltage measurements.

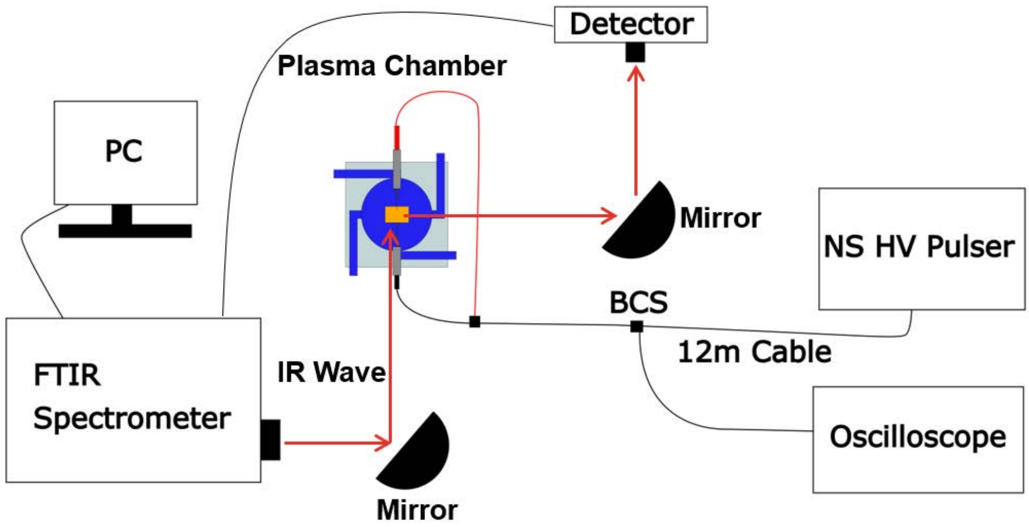

Figure 9: Sketch of the measurement setup. Red arrows show the path of the IR waves. Red cable shows the position of the driving electrode and the black the position of the grounded electrode.

Because this nanosecond pulser generates high voltages with rise times of around $\sim$ 15 ns, it produces very high noise, which interacts with nearby electrical equipment, including the FTIR. This is why the plasma and the pulser are surrounded by a Faraday cage.

3.1.4 KOH Solutions

The KOH solutions used in this work were prepared by hand. A bottle with a concentration of 0.01 mol KOH was prepared. This was done using distilled water and KOH granules. This bottle can then be used to make the desired concentrations. Using a chemical pipette, the ratio between the KOH solution and distilled water can be adjusted very precisely to obtain the desired concentration. For example, for 0.5 mM KOH, 95 ml of distilled water and 5 ml of the 0.01 mM KOH solution were mixed in a separate bottle.

3.2 Measurements

In this thesis, two different types of measurements were taken. The FTIR measurements, where a sample is placed inside the plasma chamber and the FTIR waves are guided onto it and are collected by a detector, and the energy measurements, where the voltage curve at the electrode was measured to calculate the dissipated energy.
The FTIR measurements analyzed the effects of Cu_2O reduction and were taken for different electrolytes and different applied voltages.
Every series of measurement consist of 51 measurements. The first was taken at the

beginning of the experiment. Then measurements were taken every 50 pulses, i.e. after 50 plasmas had been ignited. This equals to a total of 2500 pulse for the 51 measurement.
The different series are measured for different applied voltages. Here the electrolyte was distilled water and the applied voltage was changed from 16 kV to 20 kV and then to 24 kV. This was done for negative and positive voltages.
After that the change for different electrolyte solutions was analyzed. Here the applied voltage was kept the same with positive and negative 20 kV. The first solution was an KOH solution. The concentration of the KOH was increased for the later series. The concentration of 0.01mM KOh, 0.05mM KOH, 0.1mM KOH, 0.15mM KOH, 0.2mM KOH, 0.3mM KOH and 0.5mM KOH were used. At higher concentrations the plasma was not able to be ignited again. To ensure that the solutions were similar across the different series, the electrical conductivity was measured. This was also done for the energy measurement to see the influence of conductivity on the dissipated energy. The conductivity was measured with an GLF100 conductivity meter by GHM Messtechnik before every series of measurements. After the FTIR measurements the energy measurements were done. The measurements could not be done simultaneously because the connected oscilloscope created such EM noises, that the FTIR measurements stopped. Therefore, the energy measurements were taken separately.
For these, the voltages curves of a pulse were measured. This was done at the start and every 30 minutes to a total of 4 measurements. For the error of the energy measurements, a series was taken with 20 measurements for each time and from this the error was calculated.

3.3 Reflective Difference FTIR Measurements

There are many different ways to determine the properties of a sample. One of the most common methods is FTIR spectrometry, which stands for Fourier Transform Infrared Spectrometry. FTIR spectrometry has many advantages, one of which is that it is a non-destructive measurement. This means that the sample is not damaged by the measurement. Other advantages are that measurements can be done while the sample is still in place, often referred to as an in situ method. The principle behind FTIR measurements is that molecular bonds have a material specific vibrational energy which lies in the region of the infrared waves. FTIR uses this characteristic to determine which wavelengths are absorbed. FTIR spectrometers typically consist of 3 parts. The first part is the interferometer with an infrared light source. The interferometer sends out the IR waves in a form of an interferogram that covers a wide range of wavelengths. The interferogram is created by the integrated interferometer, where the IR waves get split into 2 parts by a beam splitter. One travels into a mirror and gets reflected back and the second also travels against a mirror, but this mirror can move so the path length of this part is adjustable(L+x). The 2 waves, with an optical retardation of 2x, meet again at the beam splitter and interfere with each other and then leave the interferometer. The accuracy depends on the minimum steps the interferometer can make to move the mirror (δx). This interferogram is then sent to the desired sample, where it is either reflected or transmitted, depending on the type of setup. The reflected/transmitted waves are directed into the second component, the detector. The detector measures the incoming EM waves and transmits the signal to the third part, the computer.

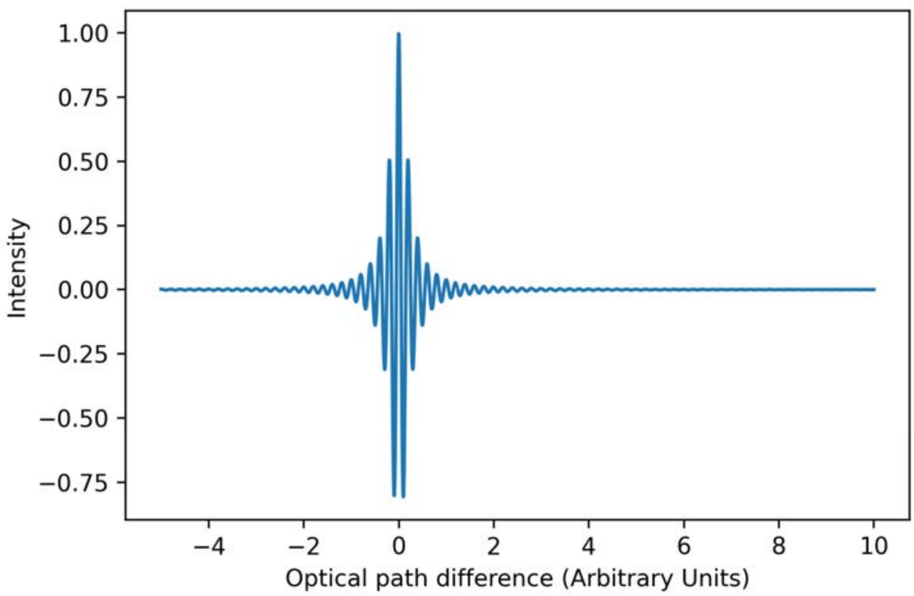

Figure 10: Example of an interferogram created by a Michelson interferometer

As the name suggest, one of the main characteristics in FTIR spectroscopy is the Fourier transformation. The incoming signal, which is the interferogram after interacting with the sample, is Fourier transformed and displayed as a spectrum. The advantage of Fourier transformation is that the whole spectrum is displayed. The peaks then indicate a present material. Typically, the Fourier transformed spectrum is displayed in wavenumbers rather than wavelengths, which is simply the number of waves per unit of length, i.e. the reciprocal of the wavelength. Also the graph is displayed from high wavenumbers on the left to small wavenumbers on the right.

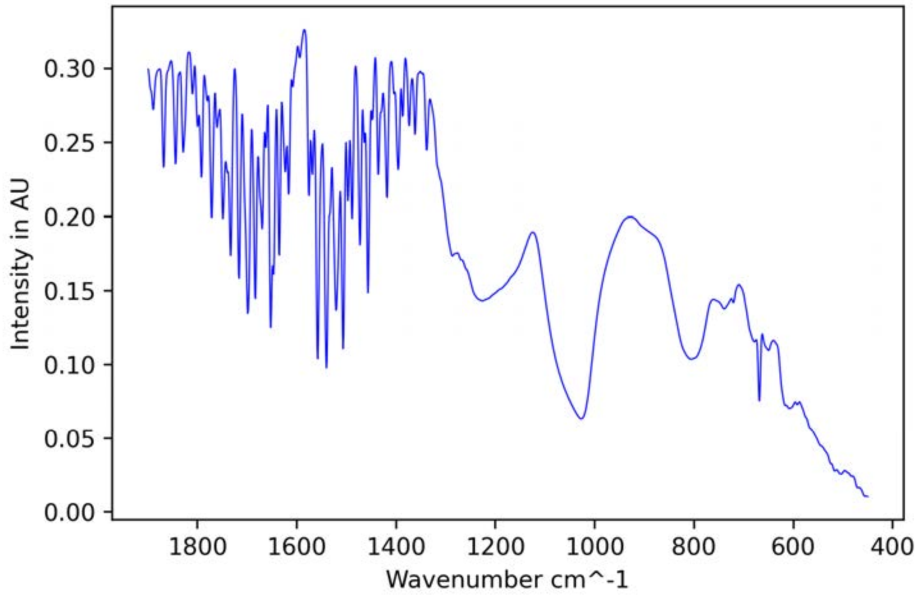

Figure 11: Example of a Fourier transformed interferogram. It is the initial spectrum of a series of measurements for a 10 nm thick copper surface deposited on an SiO_2 wafer.

As one can see in the example spectrum there are distinct peaks at certain wavenumbers. This means that a species is present, with vibrational energy corresponding to a specific wavenumber. As mentioned above, the type of FTIR measurement is reflective difference FTIR measurement. The reflective part refers to the setup. As mentioned before one way to get an interaction between the emitted IR waves and the sample can be accomplished if the electromagnetic waves are reflected at oblique angles onto the sample, so that the waves get into the sample and interact at each layer of the sample and get reflected at the backside. Then the reflected waves are guided with mirrors in an detector. As shown below, the sample is made of thin copper film which is deposited onto a silicon wafer.

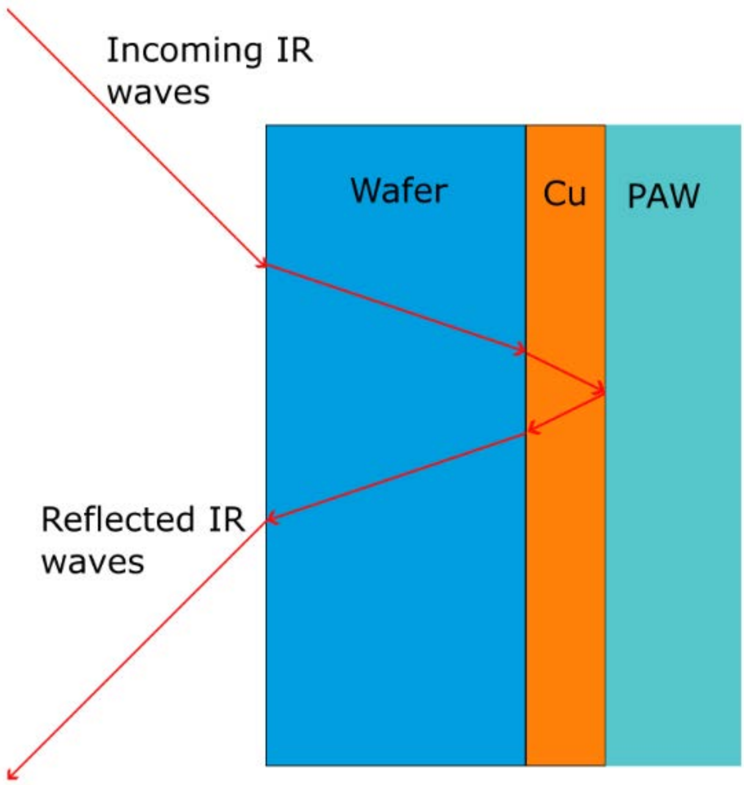

Figure 12: Sketch of the reflection of the incoming IR waves at the sample.

The "difference" in the name refers to the evaluating part of the measurement. Instead of just simply displaying a spectrum like the one shown before, the first spectrum measured is taken as the background R_0 and every spectrum measured later on will be divided by this base spectrum. This creates a line graph where it is easy to see if any difference develop. This means that if a material is enriched on the sample, a peak for $R/R_0<1$ would form on the difference graph, as more IR waves get absorbed by the material. This also means that the formation of a peak for $R/R_0>1$ indicates that specific material is being reduced in the sample and there is less on it than before. With this method one can directly see the change, and therefore whether a material becomes enriched or removed.

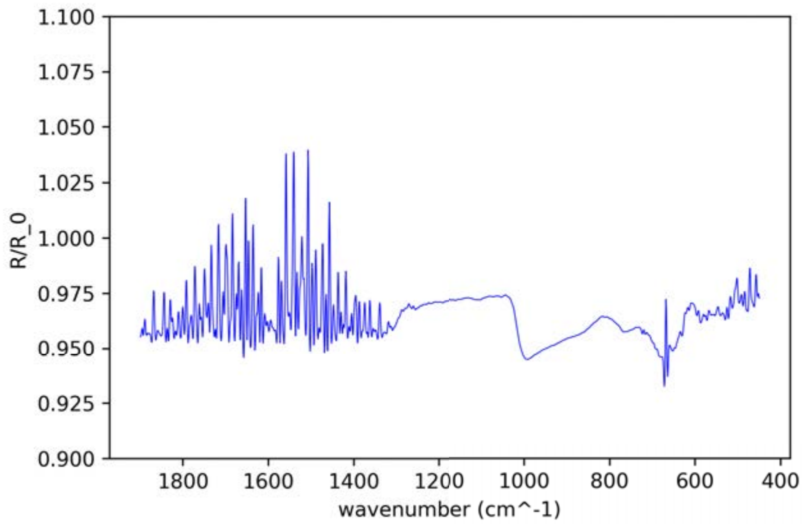

Figure 13: Example of a difference spectrum between the base spectrum R_0 and a later measurement

Although this method is useful for detecting a change of materials it is not good at determining the total amount of material in a sample. In order to obtain comparable measurements, it is necessary to obtain the same setting of variables each time. The thickness of the sample, the wafer composition and initial intensity all have an influence of the detected signal.

3.4 Dissipated Energy Measurements

To ensure that the different reaction rates for the different liquids are caused by the chemical properties and not just by change in the dissipated energy, energy measurements were taken for different liquids and also for different plasma operating times. This was done to see if the extended plasma run time changes the properties of the liquid, which might lead to a change in the ignition dissipated energy. The dissipated energy was measured using an oscilloscope and evaluated with a Python script. The oscilloscope measures the voltage curve at different times. This curve is then fed into the Python script and the voltage applied to the electrode is calculated from the applied damping of the probe. On the real voltage curve you can see 2 pulses. The first is the initial pulse and the second is the reflected pulse.

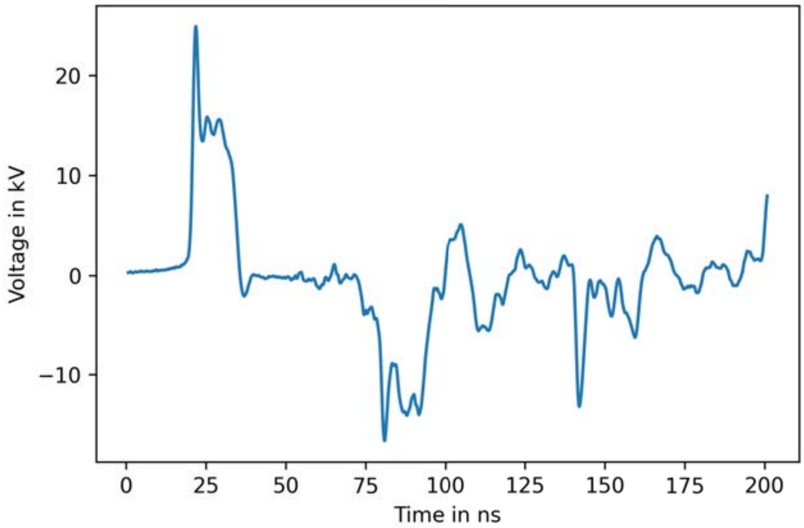

Figure 14: Example of a voltage curve. Pulse length of $\sim$ 15 ns and an amplitude of 20kV. The cable was 12 meters long.

With the python script the starting and end point of each pulse is set and since the BCS is known the current can be calculate with equation [6]

$$I = U/R \tag{6}$$

$$P = U * I \tag{7}$$

$$P = U^2/R \tag{8}$$

and with the combination of equation [7] the energy can be calculated. Now the power for both pulses is calculated and then the reflected power is subtracted from the initial power. This result is the total dissipated energy.

4 Results

In this section the results will be discussed and explained how these measurements were analyzed. First the energy measurements will be discussed, looking into the different dissipated energies for different concentrations and operating times. After the energy measurements, the FTIR measurements will be discussed, starting with the method of analysing the data, then the change in applied voltage with water as the electrolyte, and then the influence of the KOH solutions.

4.1 Dissipated Energy measurements

After analyzing the effect of plasma ignition on the Cu_2O reduction rate the dissipated energy for different electrolytes will be analyzed. The calculation is done by a python script and the values are plotted against the time. This was done for both negative and positive voltages, both are displayed in figure 16.

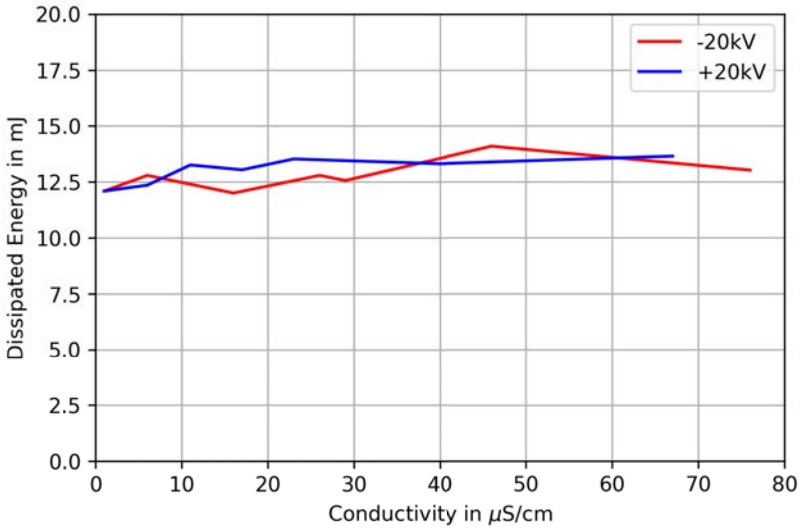

Figure 15: Plotted mean energy against the conductivity for negative and positive 20kV

The displayed error was calculated from a separate series, where for each time multiple measurements were done [Table 1].

Time	Energy/mJ										Average	Error
0 minutes	13.87	13.62	13.69	13.96	13.69	13.52	13.85	13.47	13.65	13.40	13.59	0.17
	13.42	13.56	13.53	13.69	13.40	13.38	13.46	13.60	13.75	13.39		
30 minutes	12.34	12.46	12.30	12.31	12.56	12.37	12.38	12.29	12.37	12.11	12.33	0.14
	12.40	12.37	12.50	12.24	12.17	12.22	12.46	12.27	12.52	12.01		
60 minutes	11.45	11.43	11.35	11.07	11.47	11.62	11.51	11.44	11.33	11.28	11.38	0.13
	11.14	11.32	11.32	11.35	11.54	11.28	11.37	11.29	11.42	11.58		
90 minutes	11.33	11.55	11.39	11.53	11.49	11.32	11.38	11.57	11.28	11.31	11.33	0.16
	11.37	11.38	11.31	11.11	11.14	11.26	11.32	11.47	11.16	10.87		

Table 1: Table for error calculation

These graphs show in general a small decrease in the dissipated energy the longer the plasma is ignited. Also figure 15 shows a slight increase in energy with an increase in the KOH concentration and therefore the conductivity. Figure 16 shows jumps between different series which disagree with these tendencies, even though the calculated error is low. This shows that the plasma ignition is irregular and factors like the curvature and form of the tip may have a significant influence on the dissipated energy. The increase in energy with the increase in concentration was not predicted, as the plasma glowed darker with an increase in concentration and therefore it was thought that more of the incoming pulse gets reflected.

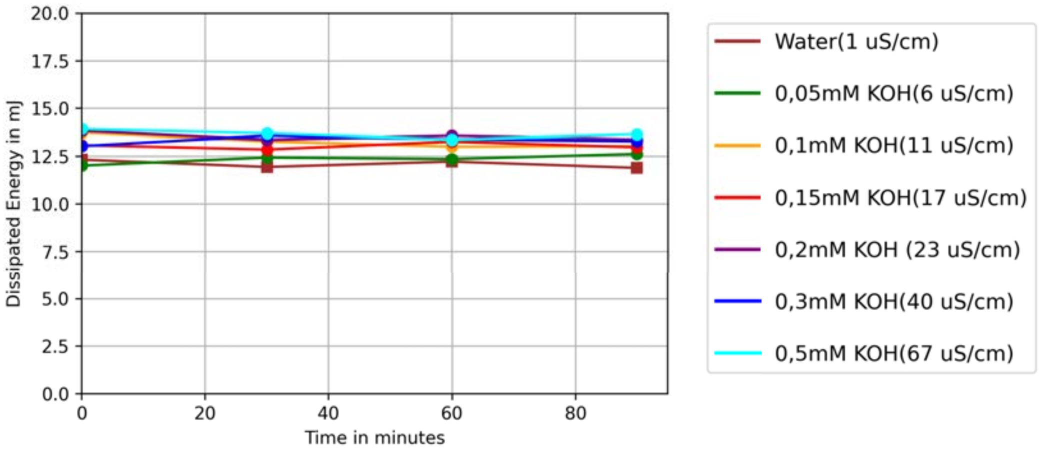

(a)

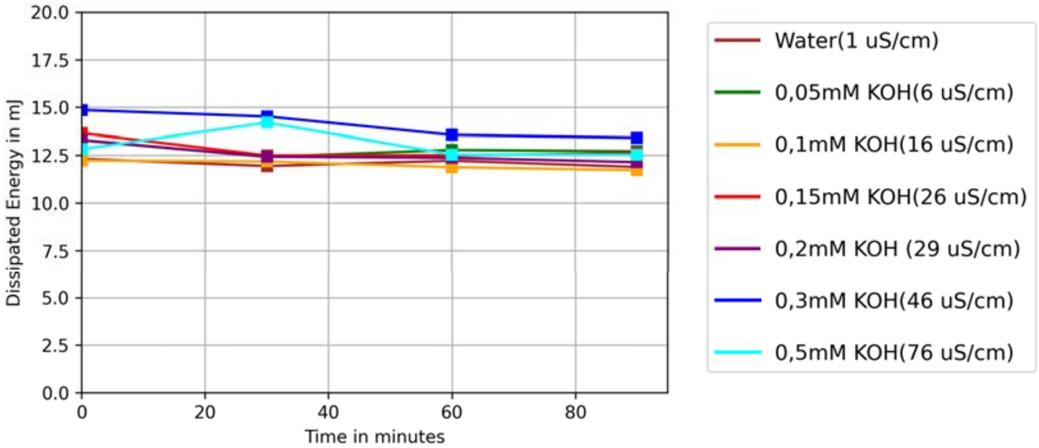

(b)

Figure 16: Dissipated energy for (a) positive 20 kV and (b) negative 20 kV.

4.2 FTIR measurements

4.2.1 Method of analyzing

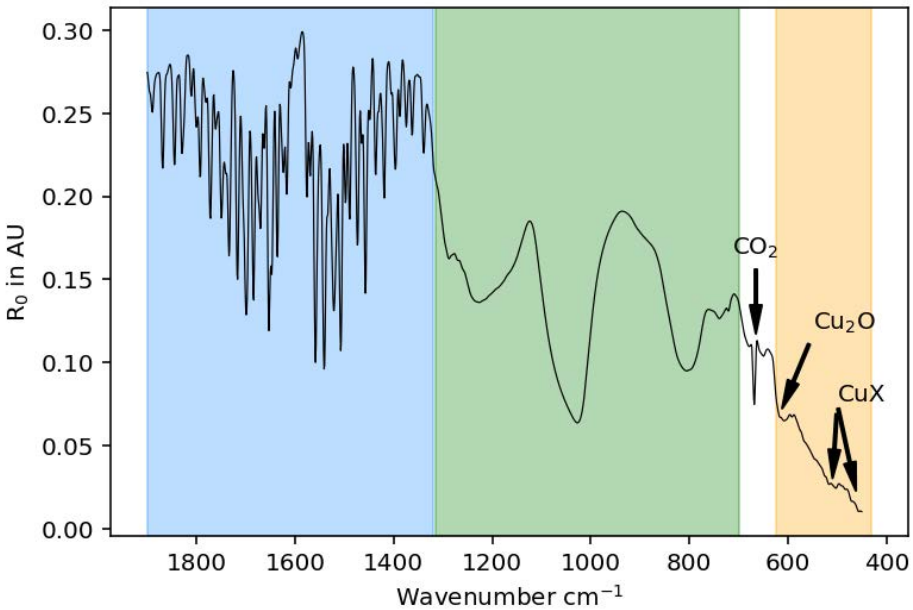

Figure 17: Spectrum of the reflective FTIR measurement on a new sample. Color blue indicates the water region, green the silicon dioxide and orange the copper region. The orange and green region together are known as the fingerprint region

As mentioned in the theoretical background, FTIR measurements result in a spectrum with peaks for different species. This results in a graph as shown in figure 17. This spectrum ranges from $\sim$ 2000 1/cm to $\sim$ 400 1/cm and can be divided into 3 segments. On the left is the first segment(color blue), where mostly water(H_2O)is present. The water comes from the ambient air in the beam path. This looks like noise and changes rapidly. Next to it in the middle is the second segment(color green). Here the distinct silicon oxide peaks are visible.
Gunde et al. [17] showed that the peak around $\sim$1250 1/cm , $\sim$1050 1/cm and $\sim$810 1/cm corresponds to silicon dioxide. The sharp peak around $\sim$670 1/cm indicates carbon dioxide(CO_2), which is present in the air around the setup [18]. Since the setup is not fully enclosed, the CO_2 peak will always be present. Next to the CO_2 peak begins the segment where the copper oxide peaks should be. Lefez et al.[19] have shown that the peak at around $\sim$600 1/cm should come from Cu_2O. Other copper bonds are located around 400 1/cm and the change of these products is not visible in this spectrum. This comes from the fact that the detector has only a range to round 400 1/cm and with the peaks being that close to the edge, the intensity and therefore the accuracy is not good enough to provide reliable results. For this reason only the Cu_2O peak will be analyzed in the FTIR measurements.

As mentioned in the theoretical background, the FTIR spectra are measured as a difference. The difference curve is used to calculate the change. While the normal difference curve is also displayed, the change in the peak that occurs on the difference curve is also analyzed.

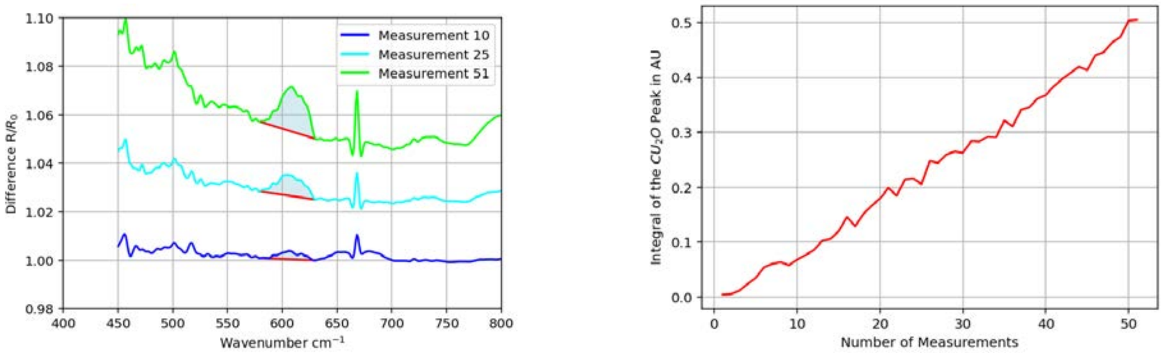

(a) (b)

Figure 18: (a) Graph of the Cu_2O peak increasing through measurements, (b) the area of the copperoxide peak plotted against the number of measurement

For this a python code was written, where the peak is integrated over a line which is drawn from the beginning of the peak to the end. The starting and endpoint of the peak were the same through all series, as the width of the peak was about the same for different series. Figure 18 displays an example for the initial difference and the graph for the integrated area. To compensate the intensity loss, which happened irregularly in different series, the later measured spectra were rescaled so the beginning and end of the peak lays on the reference of the background spectrum. With these rescaled spectra the difference was taken and then analyzed.

4.2.2 Influence of the applied voltage

This method was used to determine the influence of the applied voltage. For this, distilled water was used as the electrolyte. First the influence of the value of the applied voltage and the polarity was observed. For this, measurement series were taken for different voltages. This was done for 16 kV, 20 kV and 24 kV for both negative and positive polarities. The changes were then plotted for comparison. This is displayed in figure 19.

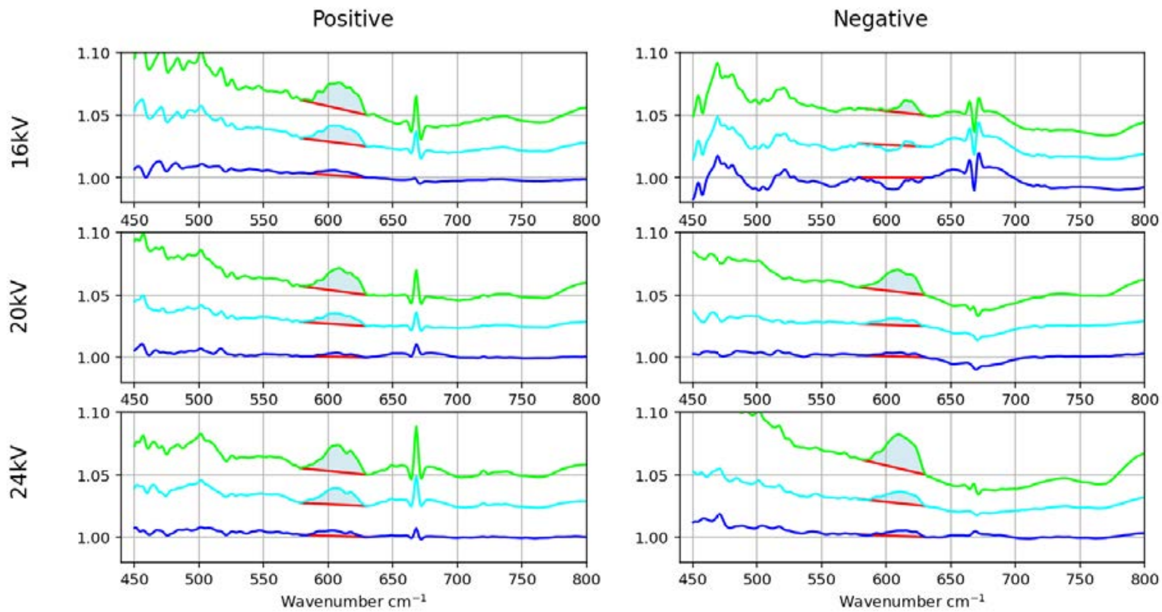

Figure 19: Display of the difference for different applied voltages. Each graph shows a different series. All series had a sample with a 10nm copper layer. Blue shows measurement 11(20 minutes after first measurement), cyan 26(50 minutes after first measurement) and the green measurement 51(100 minutes after first measurement).

The graphs 20 show different behavior for positive and negative voltages, with the positive voltages rising slightly steeper than the negative voltages at the beginning and then flattening out slightly over time. The negative voltages behave in the opposite way, rising more slowly at the beginning and then increasing with the number of plasma pulses. Negative 16 kV stands out from other negative measurements as this series

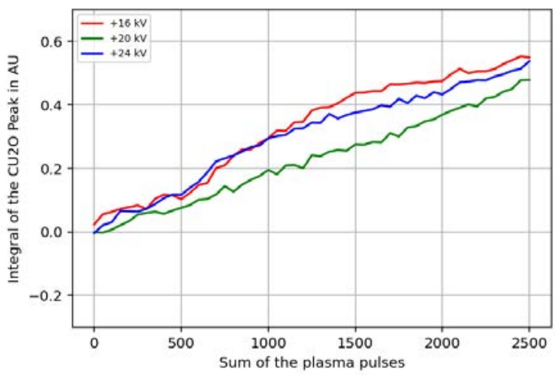

(a)

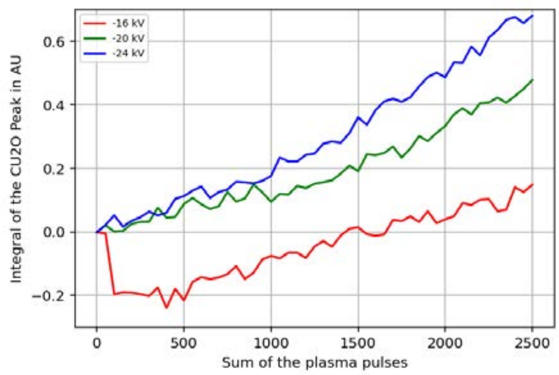

(b)

Figure 20: Plot of the integrated area for (a) positive 16 kV, 20 kV, 24kV and (b) negative 16 kV, 20 kV, 24 kV

first created a peak below the line, and therefor has a negative area, before it starts to rise again. The negative voltages also had an increase reduction for higher voltages. The positive voltages showed no such tendencies. Both negative and positive voltages show a reduction of the Cu_2O in the end. The slower start of the reduction for negative voltages may be caused from a slower removal of the copper as the copper dissolution is slower with a lower electron density and the creation of the copper nanoparticles negate the creation of the peak. This was predicted since Grosse et al. discovered a higher charge concentration for the positive voltages[11]. As the creation of the copper nanoparticles is rather slow compared to the copper dissolution the reduction catches up to the positive voltages for later measurements.

4.2.3 Influence of the KOH solution

After discovering that the applied voltage has little influence on the reduction of Cu_2O, the influence of the KOH solution was observed. This was done with the same applied voltage of 20 kV. The concentration was increased until the plasma no longer ignites. The conductivity was measured, so the starting solution had a similar conductivity as distilled water. Distilled water has a conductivity of 1 μS/cm and the starting solution of 0.01 mMol KOH has a conductivity of 2 μS/cm. The concentration of the solution was then further increased to 0.05mM KOH with a conductivity of 6 μS/cm and to 0.1mM KOH with a conductivity of 19 μS/cm. The Cu_2O reduction is displayed in figure 21 and 22.

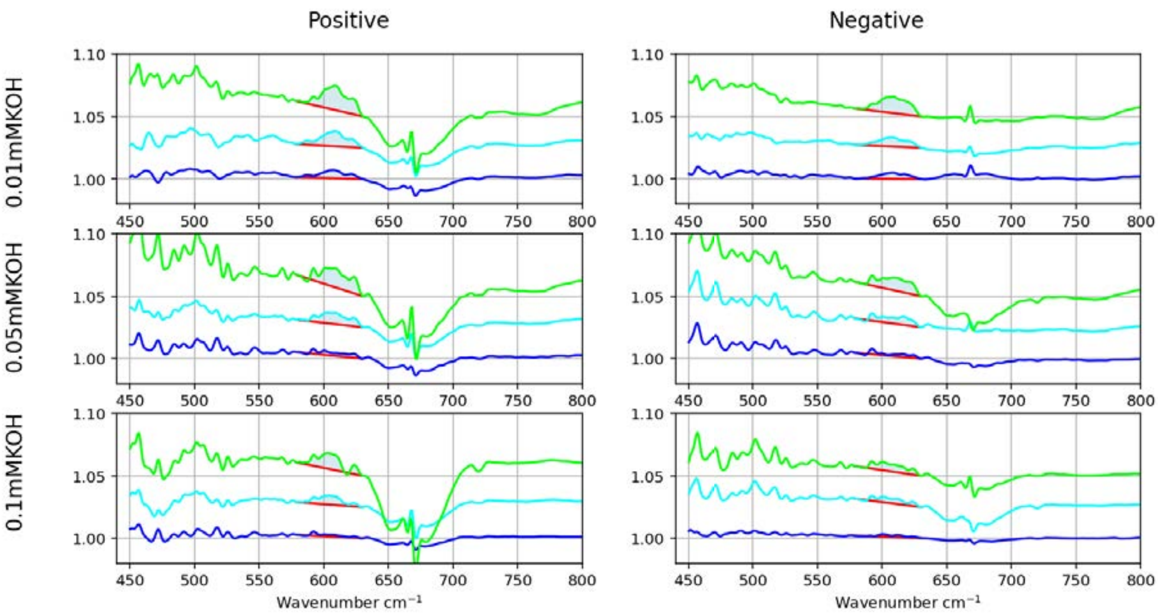

Figure 21: Display of the difference for 0.01, 0.05, 0.1 mM KOH concentrations. Each graph shows a different series. All series had a sample with a 10 nm copper layer. Blue shows measurement 11(20 minutes after first measurement), cyan 26(50 minutes after first measurement) and the green measurement 51(100 minutes after first measurement).

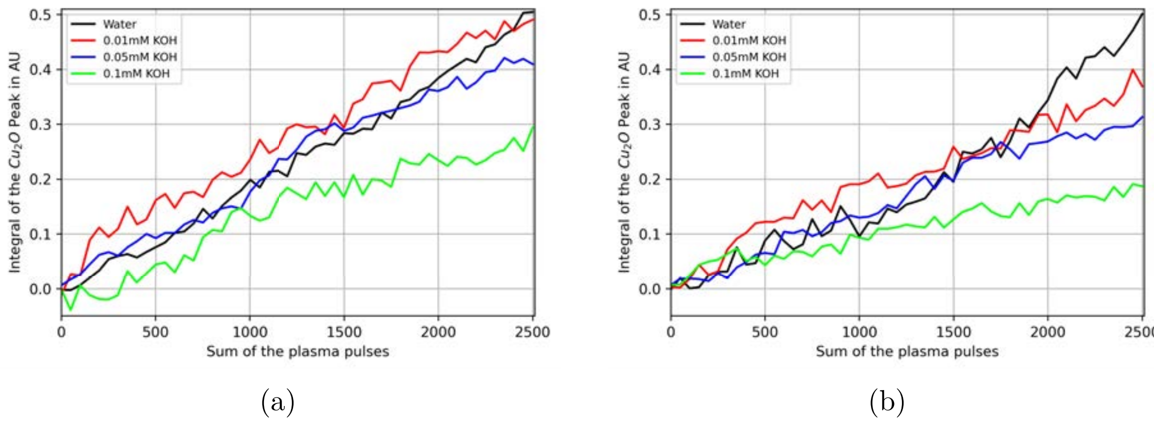

Figure 22: Graphs of the integration of the Cu_2O peak for 0.01mM KOH, 0.05mM KOH, 0.1mM KOH for (a) positive 20 kV and (b) negative 20 kV

The graphs show the tendency for the Cu_2O reduction to go down with an increasing KOH solution. The positive voltages exhibit a higher reduction rate than the negative ones. The 0.05mM KOH and the 0.1mM KOH concentration show a decline in the reduction for later measurements. This may come from the crystallization of the nanoparticle, which negate the copper dissolution and the reduction of the Cu_2O. After that the concentrations were further increased. Now the 0.15mM KOH with a conductivity of 30μS/cm, 0.2mM KOH with 41μS/cm, 0.3mM KOH with 45μS/cm and 0.5mM KOH with 76μS/cm will be analyzed. This is displayed in figure 23 and 24.

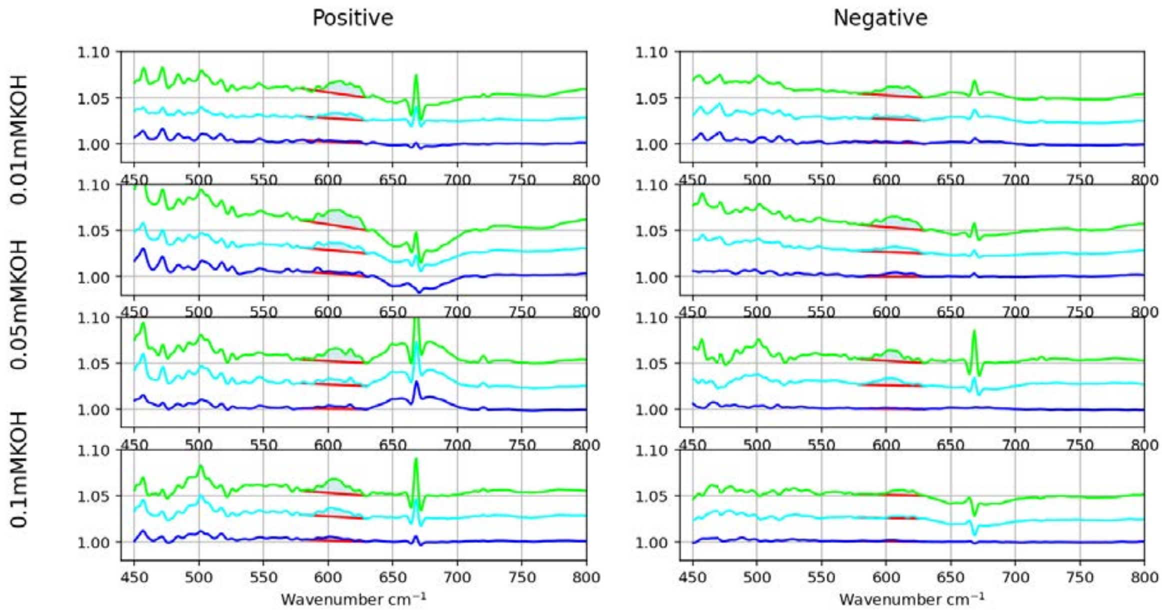

Figure 23: Display of the difference for 0.15, 0.2, 0.3, 0.5 mM KOH concentrations. Each graph shows a different series. All series had a sample with a 10 nm copper layer. Blue shows measurement 11(20 minutes after first measurement), cyan 26(50 minutes after first measurement) and the green measurement 51(100 minutes after first measurement).

The KOH solution shows no visible influence on the reduction rate of the CuO_2 but it shows a greater influence for the polarity dependency. For every solution the positive polarity has a higher reduction rate then the negative. This fits with the theory of higher electron concentration with positive voltages by Grosse et al[11] and therefore a higher copper dissolution. This probably shows that the electron and charged particles created by the plasma induce a higher reduction of the CuO_2. It is not visible whether the charged particles create additional copper bonds instead of simply reducing the material into the electrolyte, as the other copper bonds are outside of the detectors and FTIRs range. All graphs of the KOH solution and distilled water show a reduction of Cu_2O.

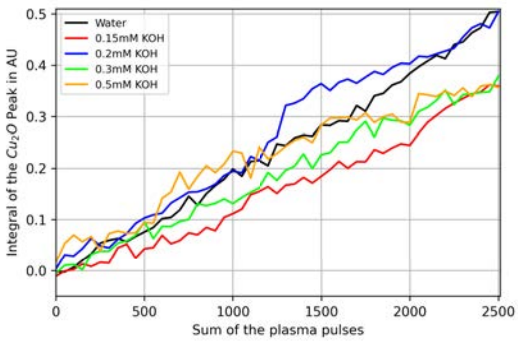

(a)

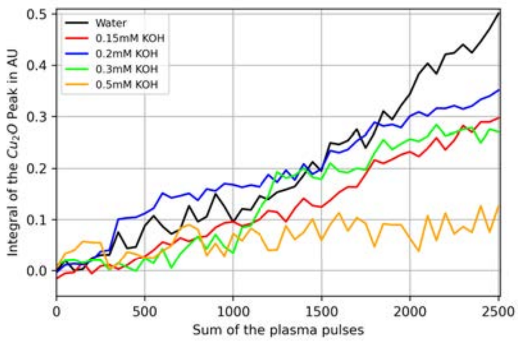

(b)

Figure 24: Graphs of the integration of the Cu_2O peak for 0.151mM KOH, 0.2mM KOH, 0.3mM KOH, 0.5mM KOH for (a) positive 20 kV and (b) negative 20 kV

It is worth noting that these graphs show a strong variation for the final reduction state. For example the negative 0.5mM KOH series only reached a reduction of ∼0.1a.u., while the positive 0.2mM KOH series reached an end reduction of ∼0.5a.u., which is 5 times higher. This may come from (i)a lower electron generation from the plasma or (ii) a higher reactiveness from the copper surface which caused a higher reduction.
As the KOH solutions are all below the water reduction one can may assume that the KOH produces more OH species, which lead to a greater CuO crystallization, or generate fewer charged particles so the copper dissolution is weakened.
After this, a separate measurement was made where the reduction rate of the Cu_2O peak was analyzed for distilled water without igniting the plasma. This series should be easily repeatable with similar results.

4.2.4 Comparison to the FTIR measurements without plasma ignition

First, the reduction rate of distilled water was measured. Here a measurement was taken every 2 minutes, which is similar to the time it took to take a measurement for 50 plasma pulses. The series was done after 51 measurements or after 100 minutes. Four different series were taken for water and then some KOH solutions were also measured. In figure 25 the reduction rate of the water is displayed.

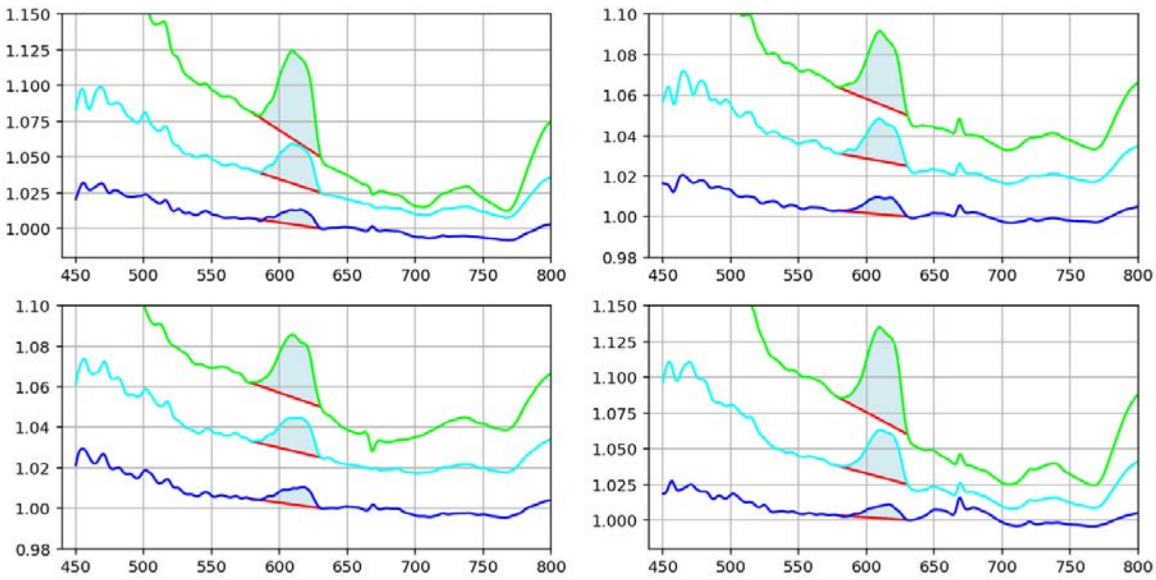

Figure 25: Display of the difference for distilled water. Each graph shows a different series. All series had a sample with a 10nm copper layer. Blue shows measurement 11(20 minutes after first measurement), cyan 26(50 minutes after first measurement) and the green measurement 51(100 minutes after first measurement).

These graphs show a higher peak than for an ignited plasma. Although the steps were exactly the same, you can see clear differences in the reductions. The difference may come from the production of the sample, as each sample is prepared on the day of the measurement. The production of the copper layer with an HiPIMPS chamber can lead to a reactive surface, which can lead to an enhanced reaction between the electrolyte and the sample and therefore affect the reduction rate. After analyzing the water reduction, these measurements were made for different KOH solutions and a H_2O_2 solution, which has a similar concentration as distilled water where a plasma was ignited for the time of one series. The KOH solutions were 0.2, 0.5 mM KOH. Those are displayed in figure 26. These graphs show a much higher reduction rate for 0.2mM KOH than for any other series. Interesting is that neither distilled water nor the 0.5mM KOH solution induces a reduction as high as the 0.2mM KOH. Either the 0.2mM KOH sample was very reactive and therefore showed a high reduction rate, or the 0.5mM KOH sample reacted with the air before treatment and is therefore not as reactive.

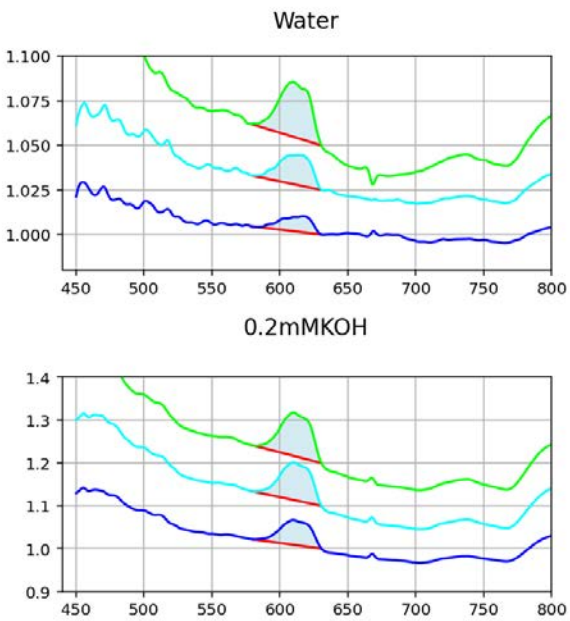

Figure 26: Display of the difference for 0.2 and 0.5 mM KOH concentrations, distilled water and H_2O_2. Each graph shows a different series. All series had a sample with a 10nm copper layer. Blue shows measurement 11(20 minutes after first measurement), cyan 26(50 minutes after first measurement) and the green measurement 51(100 minutes after first measurement).

The integrated Cu_2O peaks are displayed in figure 27. This graph shows a saturation for the 0.2mM KOH series. This saturation was seen in earlier measurements, but as the graphs have shown the saturation was not reached in other series. It also shows that the plasma has a strong effect on the Cu_2O reduction, as with the plasma ignition the reduction rate is by a factor of 5 smaller than without it. This also means that the negative voltages minimize the reduction effect more than the positives, maybe because the charged particles, which are more present at positive voltages, increase the reduction process. While the plasma produced species can also oxidize the surface, it is most likely that the electrons have the strongest influence on the reduction rate. The H_2O_2 solution had a similar reduction rate as the plasma ignited in water. This shows that the created H_2O_2 definitely has an influence on the reduction rate and the predicted concentration comes close to the concentration created by the plasma. The Cu_2O reduction also increased with time this may show that at the beginning the crystallization of the copper occurs and negate the dissolution. To summarize the ignition of a plasma has a effect to counteract the Cu_2O reduction reaction, while the negative voltages create a lower reduction rate than the positive voltages. The KOH solution has no visible influence on the reduction with an ignited plasma, but maybe as the 0.2mM KOH series has shown, the KOH solution may has an increased reduction rate without the plasma. But it could not be confirmed by the 0.5mM KOH series.

This may be attributed to the varying reactiveness of the copper layer from different samples.

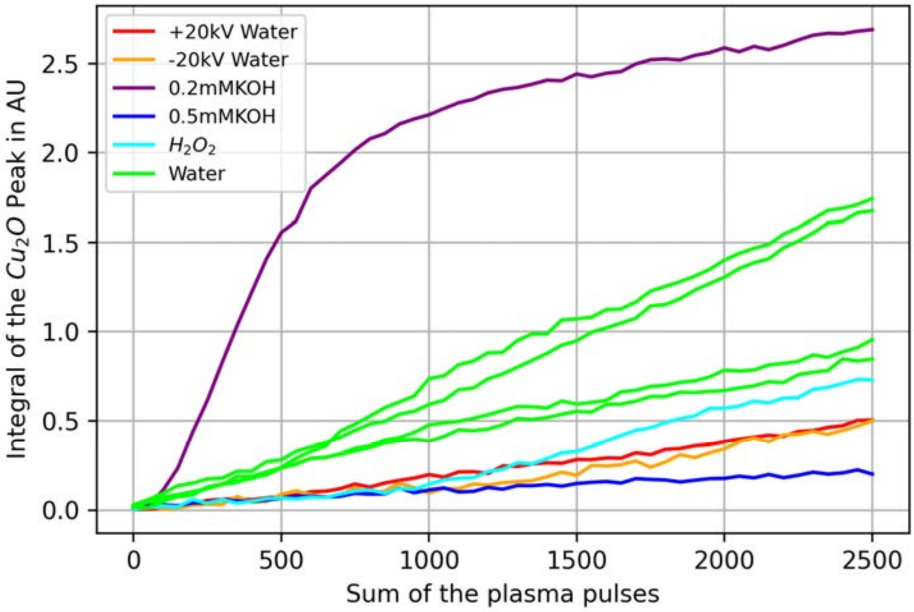

Figure 27: Graph of the integration of the Cu_2O peak for 0.2, 0.5mM KOH, water and H_2O_2 without plasma ignition. For comparison, reduction rates of the positive and negative 20kV distilled water ignited plasma are plotted.

5 Summary & Outlook

This thesis analyzed the effects of plasma ignition in different electrolytes in regard to the reduction of Cu_2O. The change of Cu_2O was measured with an FTIR and the influence of the electrolyte on the ignition was characterized by the dissipated energy measurement.
First, the dissipated energy was calculated. The graphs show a small to no influence of the KOH solution on the dissipated energy. Also often a decrease of the dissipated energy was visible for an increase treatment time of the plasma. This may be caused by the charged particles produced by the plasma, as they can lessen the electric field. Here is to say that the calculated error was rather small in comparison to the measured values. A low error and jumps in the graph show that the dissipated energy does not only depend on the conductivity but also on other parameters, like the condition of the electrode tip, which is changing throughout all the plasma ignitions.
After that the influence of the applied voltage was analyzed. As shown in figure 20 the applied voltage had a small influence on the reduction rate, as the negative voltages showed a slower start but a slight increase after some time, while the positive kept a nearly straight line. The slow start of the negative voltages was predicted as Grosse et al.[11] showed a higher electron density for positive voltages. Having established that the voltage has a small influence on the reduction, the influence of the KOH solution was observed. First low concentrations with a conductivity close to distilled water were analyzed.
At the beginning, the reduction rate was roughly the same but with an increased concentration the reduction rate started to decrease. But when the concentration was further increased the reduction began to fluctuate without showing any trend with prospect to the concentration. Even though the concentration showed no clear trend for the reduction rate, a visible difference between positive and negative voltages occurred. Every series showed a greater reduction rate for positive voltages than for negative voltages. This is in agreement with the higher electron density induced by the positive voltages.
After analyzing the influence of the KOH solutions, the FTIR measurements were compared to the reduction of copper in electrolytes without plasma ignition. This resulted in a higher reduction rate than with an ignited plasma. The water measurements showed that even though all steps taken were the same, the reduction can vary significantly. This shows that the reduction is also influenced by the reactivity of the copper layer. The H_2O_2 solution was also close to the distilled water measurements with an ignited plasma, which confirmed that H_2O_2 has an influence on the reduction rate and the calculated concentration from [15] is close to the produced H_2O_2 concentration created by the plasma.

So in conclusion one can say that the ignited plasma has an influence on the reduction of Cu_2O, and with a present KOH solution the reduction can be reduced further with negative voltages than with positive. Whether the Cu_2O dissolves into the electrolyte or the reactive species created by the plasma form different copper bonds cannot be decided from the data.
As an outlook into the future, a broader analysis of the reaction between the plasma activated liquid and the surface would be interesting. As this work only showed the reduction of Cu_2O, it did not show the reaction of different copper bonds. Also an analysis of the reactiveness of the copper layer would be good, as the measurements showed different reduction rates for the same parameters, which likely comes from the reactiveness of the mentioned copper layer. A more detailed analysis of the introduced energy would also be interesting in comparison to the properties of the tip. This could give insight into the efficiency of the plasma ignition and the influence of desired the electrolytes.

References

[1] S. Nitopi et al. "Progress and Perspectives of Electrochemical CO2 Reduction on Copper in Aqueous Electrolyte." In: *Chemical Reviews* 119.12 (2019). PMID: 31117420, pp. 7610–7672. DOI: 10.1021/acs.chemrev.8b00705 (See page 1).

[2] L. Zaza, K. Rossi, and R. Buonsanti. "Well-Defined Copper-Based Nanocatalysts for Selective Electrochemical Reduction of CO2 to C2 Products." In: *ACS Energy Letters* 7.4 (2022), pp. 1284–1291. DOI: 10.1021/acsenergylett.2c00035 (See page 1).

[3] R. Betancourt-Galindo et al. "Synthesis of Copper Nanoparticles by Thermal Decomposition and Their Antimicrobial Properties." In: *Journal of Nanomaterials* 2014.1 (2014), p. 980545. DOI: 10.1155/2014/980545 (See page 1).

[4] D. Mott, J. Galkowski, L. Wang, J. Luo, and C. Zhong. "Synthesis of Size-Controlled and Shaped Copper Nanoparticles." In: *Langmuir* Vol 23/Issue 10 (2007). DOI: 10.1021/la0635092 (See page 1).

[5] S. Popović et al. "Stability and Degradation Mechanisms of Copper-Based Catalysts for Electrochemical CO2 Reduction." In: *Angewandte Chemie* 132.35 (2020), pp. 14844–14854. DOI: 10.1002/ange.202000617 (See page 1).

[6] R. Reske, H. Mistry, F. Behafarid, B. Roldan Cuenya, and P. Strasser. "Particle Size Effects in the Catalytic Electroreduction of CO2 on Cu Nanoparticles." In: *Journal of the American Chemical Society* (2014). DOI: 10.1021/ja500328k (See page 1).

[7] P. Pottkämper and A. von Keudell. "Plasma in liquids induced modification of Cu surfaces." In: *Journal of Physics D: Applied Physics* 57.34 (May 2024), p. 345201. DOI: 10.1088/1361-6463/ad4b2d (See pages 1, 7).

[8] K. Grosse, J. Held, M. Kai, and A. von Keudell. "Nanosecond plasmas in water: ignition, cavitation and plasma parameters." In: *Plasma Sources Science and Technology* 28.8 (Aug. 2019), p. 085003. DOI: 10.1088/1361-6595/ab26fc (See pages 1, 4–6).

[9] N. V. M. Milhan et al. "Applications of Plasma-Activated Water in Dentistry: A Review." In: *International Journal of Molecular Sciences* 23.8 (2022). ISSN: 1422-0067. DOI: 10.3390/ijms23084131 (See pages 1, 3).

[10] R. Thirumdas et al. "Plasma activated water (PAW): Chemistry, physico-chemical properties, applications in food and agriculture." In: *Trends in Food Science and Technology* 77 (2018), pp. 21–31. ISSN: 0924-2244. DOI: 10.1016/j.tifs.2018.05.007 (See page 1).

[11] K. Grosse, V. Schulz-von der Gathen, and A. von Keudell. “Nanosecond pulsed discharges in distilled water: I. Continuum radiation and plasma ignition.” In: *Plasma Sources Science and Technology* 29.9 (Sept. 2020), p. 095008. DOI: `10.1088/1361-6595/aba487` (See pages 4, 5, 24, 26, 31).

[12] O. Krettek. “Investigation of Plasma-Assisted Nanoparticle Production at the Liquid-Solid Interface.” In: (2023) (See pages 4–6).

[13] K. Grosse, M. Falke, and A. von Keudell. “Ignition and propagation of nanosecond pulsed plasmas in distilled water—Negative vs positive polarity applied to a pin electrode.” In: *Journal of Applied Physics* 129.21 (June 2021), p. 213302. ISSN: 0021-8979. DOI: `10.1063/5.0045697` (See page 5).

[14] Z. Bonaventura, J. Tungli, P. Bílek, and M. Šimek. “Electron multiplication and avalanching in nanovoids at the initial stage of nanosecond discharge in liquid water.” In: *Plasma Sources Science and Technology* 30.6 (June 2021), p. 065023. DOI: `10.1088/1361-6595/abff73` (See page 5).

[15] L. Chauvet, C. Nenbangkaeo, K. Grosse, and A. von Keudell. “Chemistry in nanosecond plasmas in water.” In: *Plasma Processes and Polymers* 17.6 (2020), p. 1900192. DOI: `10.1002/ppap.201900192` (See pages 6, 31).

[16] M. Starowicz. “Electrochemical synthesis of copper oxide particles with controlled oxidation state, shape and size.” In: *Materials Research Express* 6.8 (May 2019). DOI: `10.1088/2053-1591/ab239d` (See page 7).

[17] M. K. Gunde. “Vibrational modes in amorphous silicon dioxide.” In: *Physica B: Condensed Matter* 292.3 (2000), pp. 286–295. ISSN: 0921-4526. DOI: `https://doi.org/10.1016/S0921-4526(00)00475-0` (See page 21).

[18] M. Mhanna, M. Sy, Elkhazraji, and A. et al. “A laser-based sensor for selective detection of benzene, acetylene, and carbon dioxide in the fingerprint region.” In: *Applied Physics B* (2023). DOI: `10.1007/s00340-023-08083-y` (See page 21).

[19] B. Lefez, R. Souchet, K. Kartouni, and M. Lenglet. “Infrared reflection study of CuO in thin oxide films.” In: *Thin Solid Films* 268.1 (1995), pp. 45–48. ISSN: 0040-6090. DOI: `https://doi.org/10.1016/0040-6090(95)06872-4`. URL: `https://www.sciencedirect.com/science/article/pii/0040609095068724` (See page 21).

Acknowledgements

Finally, I would like to thank all the people who have helped me through the process of writing this thesis. I want to especially thank

- Prof. Dr. Achim von Keudell, for the opportunity to write this thesis at his chair and for his support in working on and correcting the thesis.
- Pia Pottkämper for the active support in understanding the experiment and helping with questions as well as the proofreading of this thesis.
- Prof. Dr. Judith Golda for taking on the second correction.
- Steffen Schüttler for providing me with a python script to analyze the voltage curve.
- The whole EP2 chair for the warm welcome and the good times spent together.
- And the biggest thanks to my family, who have always supported me throughout my studies and motivated me to keep going.